Hindawi
International Journal of Antennas and Propagation
Volume 2018, Article ID 3903412, 17 pages
https://doi.org/10.1155/2018/3903412

Review Article

Active Surface Compensation for Large Radio Telescope Antennas

Congsi Wang ,[1,2] Haihua Li ,[1] Kang Ying,[1] Qian Xu,[3] Na Wang,[3] Baoyan Duan,[1] Wei Gao,[2] Lan Xiao,[4] and Yuhu Duan[5]

[1]*Key Laboratory of Electronic Equipment Structure Design, Ministry of Education, Xidian University, Xi'an 710071, China*
[2]*School of Civil and Environmental Engineering, University of New South Wales, Sydney, NSW 2052, Australia*
[3]*XinJiang Astronomical Observatory, China Academy of Sciences, Urumqi 830011, China*
[4]*Huawei Technologies Co. Ltd., Shenzhen 518129, China*
[5]*China Electronics Technology Group Corporation No. 39 Research Institute, Xi'an 710065, China*

Correspondence should be addressed to Congsi Wang; congsiwang@163.com and Haihua Li; haihuali_xd@163.com

Received 21 September 2017; Revised 22 December 2017; Accepted 8 February 2018; Published 29 March 2018

Academic Editor: Giorgio Montisci

With the development of radio telescope antennas with large apertures, high gain, and wide frequency bands, compensation methods, such as mechanical or electronic compensation, are obviously essential to ensure the electrical performance of antennas that work in complex environments. Since traditional compensation methods can only adjust antenna pointing but not the surface accuracy, which are limited for obtaining high surface precision and aperture efficiency, active surface adjustment has become an indispensable tool in this field. Therefore, the development process of electrical performance compensation methods for radio telescope antennas is introduced. Further, a series of analyses of the five key technologies of active surface adjustment is presented. Then, four typical large antennas that have been designed with active main reflector technology are presented and compared. Finally, future research directions and suggestions for reflector antenna compensation methods based on active surface adjustment are presented.

1. Introduction

A radio telescope is a precise instrument designed to mainly receive radio waves from celestial bodies, which can radiate electromagnetic waves. There are two primary components that make up a radio telescope: the antenna and the receiving system, in which a large aperture antenna is its main component [1, 2]. Each significant advancement in radio telescope antennas has been a milestone in the development of astronomy, without exception. As the most commonly used radio telescope antennas, reflector antennas [3, 4] can easily implement a large aperture and narrow beam, with high resolution and high sensitivity; hence, they are widely used in the fields of radio astronomy, radar, communication, and space exploration [5, 6]. In the past, the aperture of a large ground-based radio telescope antenna was usually greater than or equal to ten meters. With the rapid development of modern science and technology, the antenna design and manufacture and feeding technology have been greatly upgraded; hence, the large, medium, and small sizes of ground-based radio telescope antennas should be redefined. An antenna whose aperture is smaller than ten meters in diameter can be classified as small, an antenna whose aperture is from ten meters to thirty meters in diameter can be classified as medium-sized, an antenna whose aperture is from thirty meters to one hundred meters in diameter can be classified as large, and an antenna whose aperture is larger than one hundred meters in diameter can be classified as ultra-large. So far, more than twenty large and medium-sized radio telescopes have been built around the globe in various forms [7–9], including fixed single-aperture spherical radio telescopes, non fully steerable standard parabolic radio telescopes, fully steerable antenna-shaped radio telescopes, and telescope arrays. A large radio telescope (hereinafter referred to as a "large antenna") operating in a complex environment is affected by gravity, temperature, wind, and other factors, which lead to structure distortion. Further, there are random errors related to manufacture, installation, and so on. These factors together result in reflector surface deformation of the antenna, which degrades surface accuracy and electric performance through gain loss, pointing error, and sidelobe degradation [10–17]. Therefore, it is necessary to adjust the antenna structure and shape to compensate for the loss of electric performance.

For this purpose, the paper discusses the development process of electric performance compensation methods for radio telescopes, presents the characteristics of large antennas with the application of the active surface adjustment, summarizes the key active adjustment technologies, compares typical large antennas using active adjustment for the antenna main reflectors, and eventually discusses the structure design program and research proposal for active surface compensation of the QiTai Telescope (QTT) antenna in Xinjiang, China. The presented content provides a technical reference for performance assurance and improvement of ultra-large radio telescopes.

2. Development History of Performance Compensation for Radio Telescope Antennas

According to the classical Ruze formula [18], antenna technicians thought that the most critical issue was to ensure the surface accuracy for satisfactory electric performance of radio telescope antenna. Futhermore, under situation of the same antenna efficiency, it is becoming more and more difficult for large-aperture high-frequency antennas to achieve an acceptable machined surface on account of the extremely demanding surface accuracy requirements.

Later, to reduce the difficulty of panel processing, antenna designers adopted not only rigid materials for antenna fabrication, but also precise antenna structure design strategies, such as "homologous design" [19, 20], to improve the main surface deformation at various elevations and ensure electric performance. For large antennas in operation, the frequently used methods for compensating electric performance include mechanical and electronic compensation techniques, among other approaches [21]. Mechanical compensation techniques include main reflector, subreflector, and deformable plate compensation. Electronic compensation mostly refers to feed array compensation. A comparative analysis of various compensation methods shows that the main reflector compensation method is the best option, which can provide the best integrated performance. The subreflector compensation method can generate good results when the structural distortion is not very grave, and deformable plate compensation can improve antenna performance to a certain extent. Although the shape of the main reflector and subreflector cannot be changed, the array feed can partly compensate structural distortion. Finally, the compensation effect of multiple methods combined is better than that of one method alone.

To satisfy the development needs of radio astronomy, antenna apertures have become larger, the working frequencies higher, and antenna structures more complex, which makes antenna aperture efficiency and pointing more sensitive to structural deformation. However, the traditional compensation methods can only adjust the reflector antennas in azimuth and elevation. Since a single panel of the main reflector is not adjustable, the surface accuracy of the reflector cannot be adjusted using only traditional compensation methods. The traditional compensation methods first calculate the best fitting surface after the deformation of the main reflector and then adjust the azimuth and elevation of the reflector to, respectively, move the main reflector to the best fit surface and the subreflector to the matching position of the best fit surface. In light of the changes, traditional compensation methods, such as moving the main reflector and subreflector to the matching positions of the best-fit paraboloid, are ineffective. The surface shape of the main reflector must be adjusted, which is to say that the antenna electric performance will be compensated by realizing active adjustment of the main reflector. As shown in Figure 1, to further improve antenna surface accuracy, a variety of surface shape control methods are proposed in the design and manufacture period of large antennas [22–25], such as rigid design, homology design, radome or package handling, and optimum presetting angle installation. Up to now, all large antennas in the gigahertz band worldwide have been integrated with rigid design, structural homologous design, and the active surface adjustment to ensure that the antenna surface accuracy reaches the millimeter level. Therefore, active surface design is the trend in antenna construction, which is also an important technique to realize high steering accuracy.

3. Active Surface Compensation Technology System

During observation periods, an antenna is influenced by complex environmental factors. With changes in the antenna's azimuth and elevation attitude, the antenna surface topography changes in real time. It is imperative to adopt active adjustment for large antennas operating at high frequencies [26, 27].

Figure 2 presents the realization process of the active surface adjustment of large antennas. As a large antenna is observing, its surface is measured in real time by modern surface detection technology. Then, the actual surface deformation information is transferred to the main control computer, which can provide the panel adjustment amount through a certain mathematical algorithm. Next, the control network of the active surface control system will adjust actuators in various positions to make mechanical motions by remote control. Thus, the position of each reflector panel can be fine adjusted, and eventually the surface shape of the antenna will be corrected. In combination with the development history of large antennas and the application status of the active surface, this paper summarizes key technologies for realizing active surface compensation, including calculation of the amount of surface adjustment, segment design of the active main reflector, actuator design, active surface control, and surface detection. Based on the analysis above, we present the basic principles, difficulties, and application ranges of these key technologies.

3.1. Actuator Design. The actuator is the point at which active surface adjustment is implemented, and it is the main mechanical adjustment device in the reflector shape control

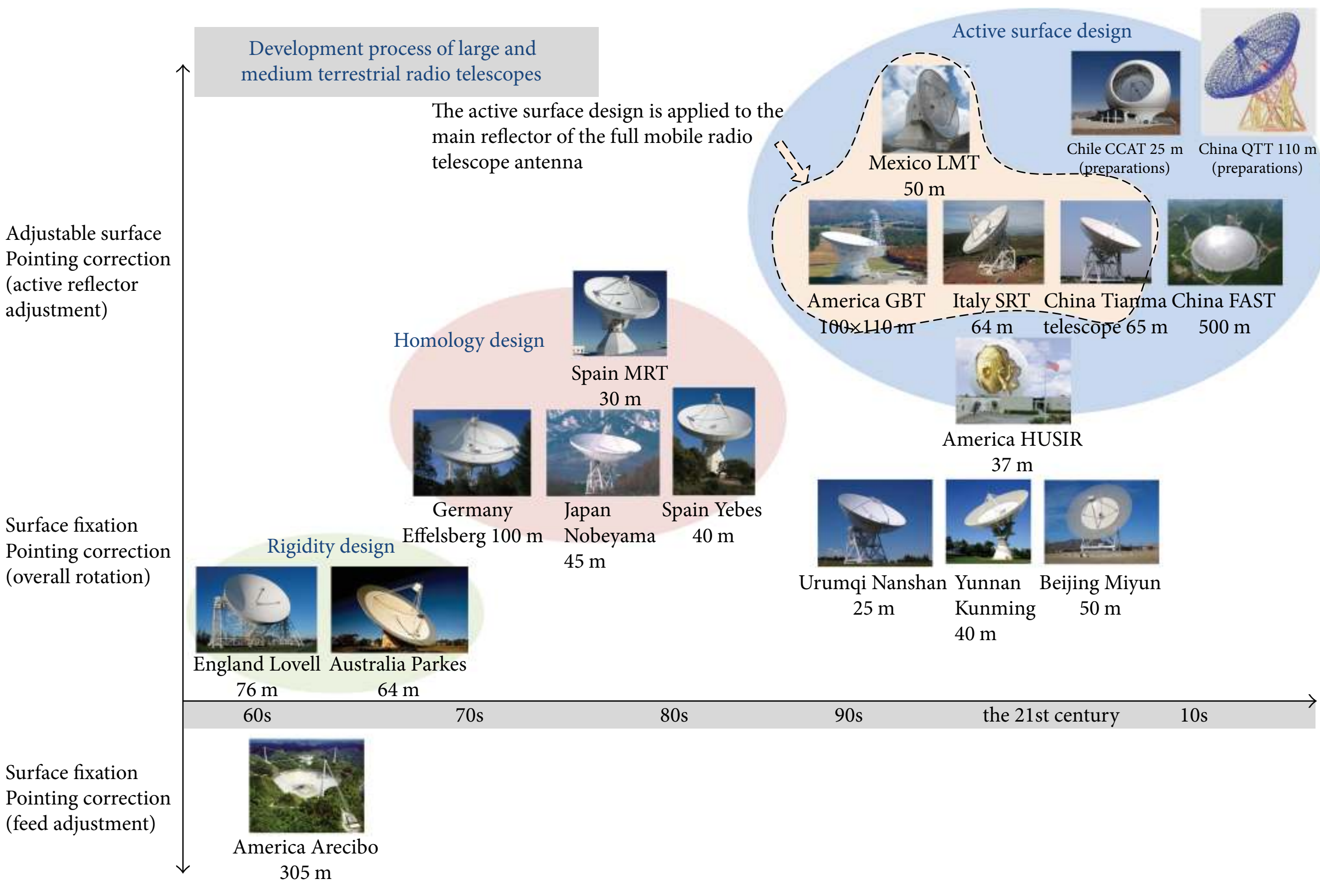

Figure 1: Development history of radio telescopes.

of large antennas. Actuator design refers to the mechanical structure design of the actuator, whose three key indexes are weight, stroke, and adjustment accuracy. A series of studies have been carried out [28, 29] on the design, simulation, manufacturing, and testing of actuators. To achieve the real-time requirements of active surface adjustment, it is necessary to ensure that the actuator is capable of fast response, precise positioning, and sufficient stroke. Further, high reliability, strong anti-interference capability, and long service life under severe working conditions must be guaranteed over a wide temperature range. With the development of modern precision instruments, piezoelectric, electrostrictive, magnetostrictive, shape-memory alloy, and electrorheological fluid actuators are most commonly used.

It is understood that dozens of actuators are out of order and need to be repaired or replaced for the GBT antenna of the United States every winter. In consideration of the personal safety of the staff and practical engineering problems related to mass production and cost, the QTT antenna actuator design still needs to be improved. They should be designed to be small and light, to have a long service life, and to have reliability and adaptability in a low-temperature environment. Therefore, it is suggested that the QTT antenna actuators should adopt a stepping motor and the light screw design, with a precision sensor design scheme, which should be supplemented by deicing and low-temperature resistance sealing measures to ensure robust operation under the conditions of the Qitai observatory environment. Of course, the electromagnetic compatibility (EMC) problem must be taken into consideration.

3.2. Active Surface Control System. An active surface control system is fundamental to achieving active surface adjustment, which belongs to a subsystem of the antenna control system. It comprises a slave computer, actuators, a control bus, a power supply unit, and other parts, and the control bus, which links to and controls the actuator, constitutes the whole control network. A previous study was conducted [30, 31] of the control system wiring, motor, communication protocol, actuators, and so on. The control system wiring is very important. The simpler the route is, the lesser the burden on the antenna structure is, which improves the control response time and reduces the signal loss.

According to the various factors that cause deformation of the main reflector, there are three main types of active surface control systems at present. The first is the open-loop correction control system based on the structural finite element model, which focuses on gravity deformation. For example, the SRT 64 m of Italy [32] stores the antenna compensation information corresponding to self-weight deformation inside the database beforehand, to achieve real-time compensation though a kind of lookup table during antenna operation. The second is a half-closed-loop correction control system based on temperature measurement and the finite element

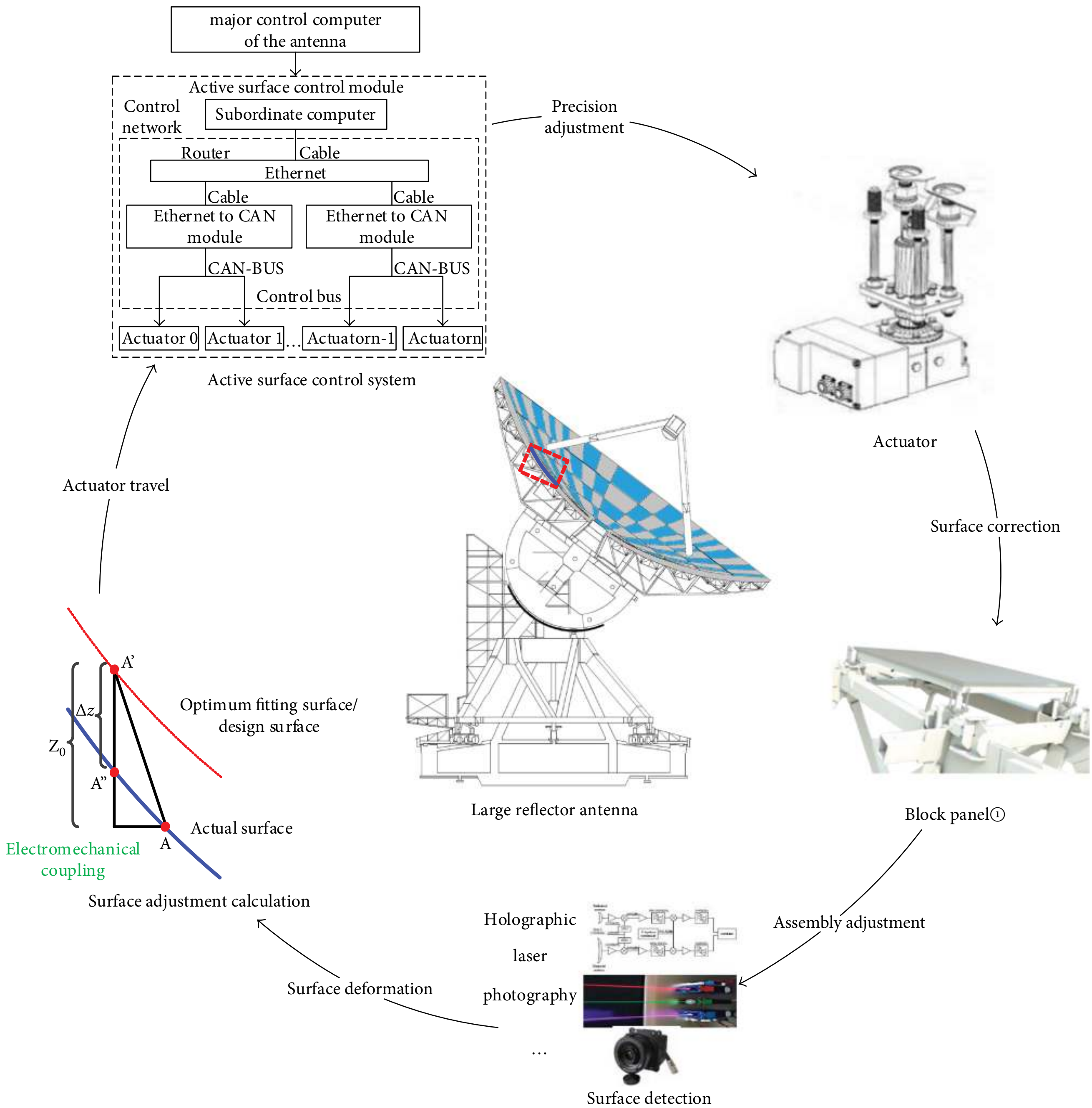

Figure 2: Process of active surface adjustment of large antennas.

model to address thermal deformation. For instance, Tianma 65 m of China carried out active compensation for temperature deformation, to compensate for the large temperature difference at night in 2016 [33]. The third type is a quasi-real-time closed-loop control system based on large-scale surface measurement techniques (including holographic measurement). In particular, the American GBT antenna had applied the partial focus holographic measurement technique [34]. However, due to the limitation of measurement time and accuracy (ultra-large antenna aperture), as well as the speed of control response (a great number of control units), the active surface control system is still unable to achieve fully real-time closed-loop control. It is proposed that, for the QTT antenna, in-depth studies should be continued regarding compensation database establishment, the rapid detection and accurate inversion of the reflector surface, actuator response time, and so on.

3.3. Surface Shape Detection. Surface calibration and real-time measurement of the antenna reflector is the first step towards the implementation of active surface adjustment. Generally, the measurement accuracy must reach 1/3 to 1/5 of large antenna surface error specification. On account of the large aperture and high surface accuracy of

Table 1: Traditional methods of antenna surface measurement.

Methods		Measurement accuracy/mm	Scope of application
Mechanics	Template method	±0.1~0.2	It is only suitable to measure the antenna in elevation and more effective for the installation and detection of small and medium antennas.
	Lathe method	±0.02~0.1	It is only suitable for measuring small antennas (the diameter should be less than or equal to 4 m).
Optics	Theodolite and steel tape method	<±0.2	It is widely used.
	Double pentaprism method	±0.15~0.66	It can measure the surface accuracy of paraboloid at different elevation angles.
Others	Pentaprism and tape method, steel wire ranging method, car measurement method, etc.		

Table 2: Modern antenna surface measurement methods.

Measurement methods	Characteristics	Remarks
Theodolite method	Less than 20 m under the accuracy 0.2 mm	The measurement process of large antennas is slow.
Total station method	Less than 120 m under the accuracy 0.2 mm	Compared with the former, it possesses lower cost, easier operation, faster construction of the coordinate system, and faster maintenance time.
Photogrammetric method	Less than 125 m under the accuracy 0.2 mm	It utilizes object images to reconstruct 3D shapes.
Laser tracking method	Less than 400 m under the accuracy 0.2 mm	It needs to be recalibrated when the instrument tilts, and dense sampling is slow.
Phase retrieval method	Tianma 65 m adopts this method to obtain the surface precision 510 μm.	It uses a single receiver and an astronomical source to measure the beam at a couple of different secondary focus positions.
Tower holography method	ALMA telescope, which is a reflector antenna array made up of antennas with the aperture of 12 meter and 7 meter, adopts this method to obtain the surface precision better than 20 μm.	It is a near-field measurement method using a tower transmitter.
Radio holography method	GBT adopted this method to obtain the surface precision 0.46 mm.	It requires a second reference telescope or receiver system, and both the telescope and receivers must have good phase stability.
Edge sensor method	Good stability and sensitivity on the order of 10 mm and CCAT use this method	It measures the real-time changes of panel-to-panel in the surface to implement real-time closed-loop control of the surface during astronomical observations.

an antenna, surface detection technology of the reflector is very demanding.

In the past, before the appearance of the active surface adjustment, surface detection was mainly used in the initial stages of panel manufacturing, installation, and debugging. Traditional measurement methods mainly include mechanical, optical, and electrical methods [35], as shown in Table 1. The main characteristics of these methods include small range, low accuracy, slow measurement speed, low level of automation, great labour intensity, and the limitation of antenna attitude.

Since the 1980s, many modern precision measuring instruments have been developed, which have allowed tremendous advances in antenna surface detection methods. The modern antenna surface detection methods [36], as shown in Table 2, can offer greater flexibility, as will be presented in this section.

3.3.1. Theodolite Method. More than two high-precision electronic theodolites are applied with other accessories and system software to make noncontact measurements of the antenna by the principle of forward intersection of the space angle [37], which is widely used in the manufacturing industry for antennas.

3.3.2. Total Station Method. This method uses a high-precision total station with ranging marks, such as reflective films, to measure the antenna reflector based on the measuring principle of the polar coordinate. For example, the installation and measurement of GBT panels were made by applying the total station and theodolite methods to achieve the surface precision of 1.1 mm.

3.3.3. Photogrammetric Method. One or more high-precision measuring cameras are used to make rapid noncontact measurements based on the principle of intersection measurement [38], which is especially suitable for a dynamic measurement field. For instance, when the United States Arecibo telescope was upgraded to increase its working frequency from 600 MHz to 10 GHz [39], the photogrammetric method was used so that the surface accuracy would be superior to 2 mm after panel adjustment.

3.3.4. Laser-Tracking Method. The measurement principle of the laser-tracking method is the same as that of the total station method, which applies a single laser tracker and makes fast tracking measurements by the measuring principle of the polar coordinates [40]. It has a high measuring precision of up to 100 μm within a 200 m range and a high measuring speed of up to 5 zones per second.

3.3.5. Radio Holography Method. Taking advantage of the Fourier transform relationship between the far-field pattern and the aperture field distribution of the antenna, the far-field pattern is measured to deduce the antenna aperture field distribution reversely including the amplitude and phase. Then the antenna surface deformation information is obtained through the geometrical optics method [41]. This method can be applied without any additional equipment. Moreover, it has the advantages that it can be conducted in real time with high precision, high automation, noncontact, nondestruction, and unlimited range with simple devices and no special requirement for antenna attitude. For example, GBT adopted the radio holography method when equipped with a reference receiver, together with the theodolite and total station methods, to evaluate the surface with an accuracy range from 1.1 mm to 0.46 mm [42].

In addition, the phase retrieval method is used to measure the amplitude of multiple far fields, and the near-field holography method, or called as tower holography method, is for measuring the amplitude and phase of near fields in antenna surface measurement. The former was widely used in the early years, with convenient measurements but low accuracy. In comparison, the latter has gradually become popular in recent years, and it achieves high measurement accuracy; however, the requirement for a tower transmitter makes it unsuitable for large aperture antennas. The radio holography method has a high measurement precision using a reference telescope or receiver which is time-consuming and cost-consuming. A novel method proposed for CCAT that uses stiff and thermally stable panels (typically CFRP panels) and edge sensors can measure the real-time changes of panel-to-panel in the surface with the relative low cost [43]. In conclusion, the radio holography and edge sensor seem to be the most appropriate method for measuring the surface topography of the QTT antenna. Certainly, a wide and diverse range of measuring methods can be adopted to enhance the accuracy of surface measurement during operation in high-frequency bands.

3.4. Calculation of Amount of Surface Adjustment. Calculation of the amount of surface adjustment is central to active surface modification, which can be obtained by both structural model simulation and reflector surface morphology measurement. The former needs to be stored in the database of the control system in advance. Hundreds of panels usually make up the main reflector of a large antenna, and there are always some position errors between the fabricated surface of the reflector and the ideal design surface of the reflector. In [44], an adjustment calculation method was presented which takes the best-fit surface as the target surface. The research team of Xidian University has conducted extensive relevant research on the determination of panel adjustment on the basis of microwave antenna electromechanical coupling [10, 45–47]. These methods can theoretically optimise antenna surface accuracy by only one time adjustment, but most of them are used for installation and debugging before antenna operation begins.

The panel adjustment strategy of the active surface is similar to the basic idea of the “best adjustment amount,” described above. The calculation method is iterative, but the difference is how electric performance compensation can be realized quickly. The studies reported in [47–51] conducted optimization analyses of structural parameters of support trusses and feed illumination parameters in relation to surface accuracy, gain, and beam pointing as the design objectives. In addition, shared actuators are generally adopted among four segment panels of the active surface to reduce the number of actuators [52]. In this context, the adjustment amount coupling of adjacent panels must be taken into account. To improve the beam pointing and antenna gain, the authors proposed an electromechanical coupling calculation method of the active surface adjustment amount [53] of large reflector antennas. This method first establishes and modifies the finite element model of the antenna structure and then determines the corresponding target surface through panel movement and fitting adjustment, overall reflector surface precision adjustment, as well as panel fitting, and rotation adjustment to calculate the best adjustment amount of the actuators quickly. This method can adjust the surface to either a shaped reflector surface or to a normal parabolic surface using the same panels.

In using this method, the finite element model of an antenna structure, comprising a pedestal, centre body, back-up frame, and reflector, can be modified carefully little by little with the actual measurement data. In addition, the installation position error of every panel in the active reflector and the initial stroke of the actuator need to be measured and recorded, and these predetermined deviations should be eliminated in the adjustment calculation method.

4. Active Surface Compensation Status of Typical International Telescopes

Many large-scale radio telescopes have been built around the world, directly using or upgrading to active surface adjustment, such as GBT, LMT, HUSIR, Effelsberg, and SRT, as well as FAST and Tianma in China [54–61]. The main parameters of the above-mentioned antennas are listed in Table 3. According to the analysis of these radio telescopes, there are only four international large-scale fully steerable radio telescopes that have adopted an active main reflector design, namely, the GBT in the United States, the LMT in Mexico, the SRT in Italy, and the Tianma telescope in China. Table 4 presents the related parameters of active surfaces of these four large-scale antennas. The application status of the active surface adjustment of these four typical antennas will be further analysed below.

Table 3: Typical radio telescopes with active surface.

Name	Aperture/m	Total mass/t	Frequency/GHz	Surface accuracy/mm	Pointing precision/(")	Year of work	Remarks
GBT	100 × 110	7856	0.1–116	0.24	1.5	2000	America
LMT	50	800	75–350	0.075	1.08	2008	America, Mexico
HUSIR	37	340	85–115	0.1	3.6	2010	America; adjustable secondary reflector
Effelsberg	100	3200	0.395–95	1	10	1972	Germany; adjustable secondary reflector
SRT	64	3000	0.3–115	0.15	5	2011	Italy
Tianma	65	2640	1.25–46 (L/S/C/X/Ku/K/Ka/Q)	0.3	3	2012	China
FAST	500	30 (feed cabin)	70 MHz–3 GHz	1-2	4	2016	China

Table 4: Four radio telescopes with active main surface.

Name	Forms of main reflectors	Surface accuracy (mm)	Number of blocks	Types of panels	Shapes of panels	Manufacturing accuracy of single panel (μm)	Number of actuators
GBT	Offset Gregorian	0.24	2004	44 rings	Trapezoid	68	2209
LMT	Standard Cassegrain	0.075	180	5 rings	Irregular quadrilateral (combination)	<40	720
SRT	Shaped Gregorian	0.15	1008	14 rings	Trapezoid	<65	1116
Tianma	Shaped Cassegrain	0.3	1008	14 rings	Trapezoid	<130	1104

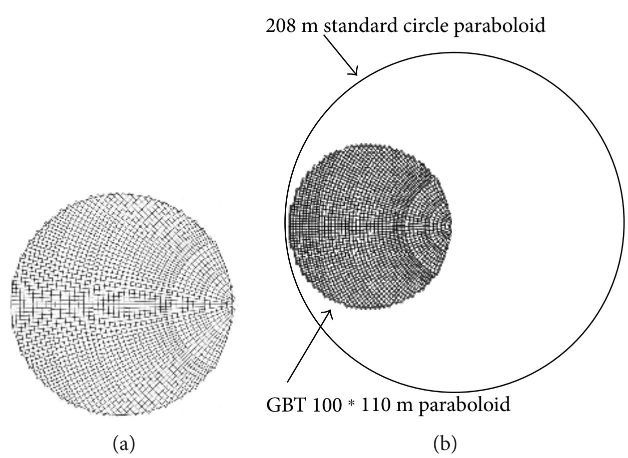

Figure 3: Segment design of GBT main surface [60]. (a) Main surface of GBT and (b) parent paraboloid of GBT.

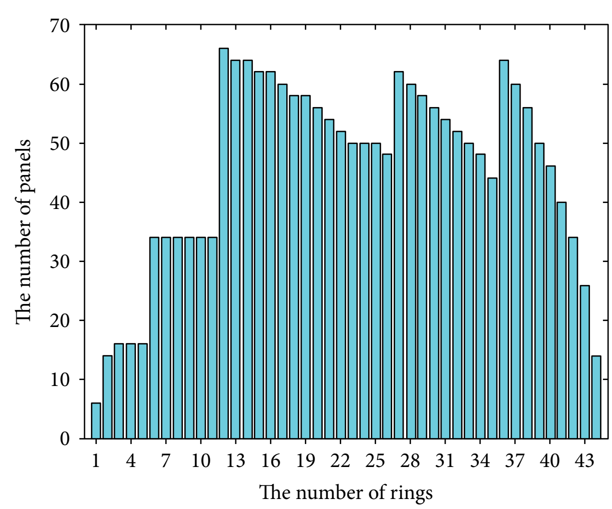

Figure 4: Number of panels in each ring of the GBT main surface.

4.1. Green Bank Telescope. The active surface adjustment of the GBT mainly addresses structural deformation caused by self-weight [62]. Because the high-frequency observations are done only at night, thermal deformation of the telescope structure caused by solar radiation can be simply avoided. The antenna surface accuracy can be up to 0.24 mm after adjustment of the active surface.

4.1.1. Segment Design. The segment design of the main reflector of the GBT [63], as shown in Figure 3(b), is based on a 208-meter standard circle paraboloid and the division form of hoop/radial annularity on a circle paraboloid. Since the main reflector of the GBT is only part of the circle paraboloid, the whole antenna aperture is elliptical, and the hoop part of each panel is only part of the ring as well. The panel of the whole active reflector presents radial distribution from one end of the reflector to the other, and it exhibits a kind of form that is "less at both ends and more in the centre" as seen in Figure 3(a). The numbers of panels in the various rings of the main reflector of the GBT are given in Figure 4, and the main reflector is divided into 44 rings along the radial direction comprising 2004 panels in total. Some of the 44 rings are designed with panels of the same type, which can be manufactured by the same mould; the 44 rings are composed of a total of 16 kinds of panels. This means that only 16 kinds of moulds are required for the fabrication of all of the panels, which can greatly reduce the processing cost, but produces

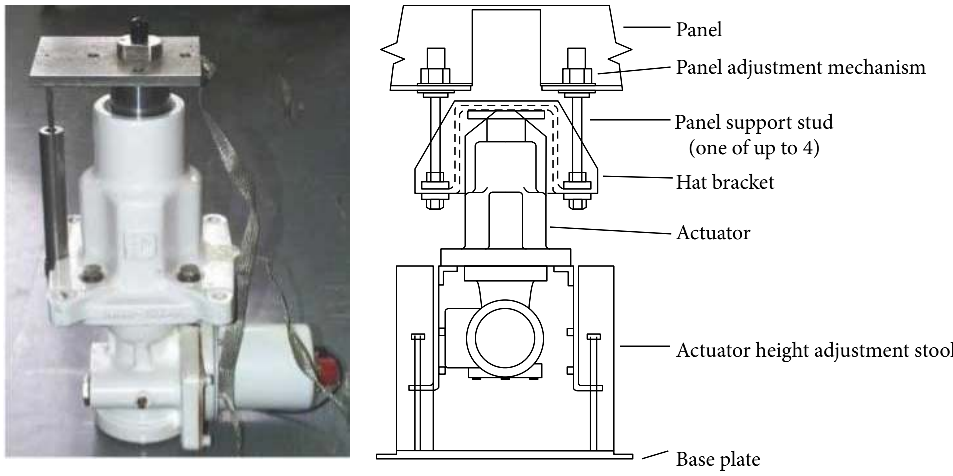

(a) Physical photo (b) Mechanical configuration

Figure 5: GBT actuator [63].

Table 5: Design parameters of GBT actuators.

Stroke	51 cm
Positioning accuracy	25 μm
Speed	250 μm/s
Static load	481 kg
Dynamic load	186 kg
Service life	20 years, 1270 meters per year
Type of motor	DC brush motor
Position sensor	Linear variable differential transformer (LVDT)

the principle errors between the panel and the design surface. The GBT panels are composed of an aluminium surface layer and an aluminium reinforced rib frame. The radial length of a single segment panel is approximately 2.5 m, and the width is 2 m. The corresponding average area is approximately 3.9 m^2. The surface accuracy of each panel is approximately 68 μm, and the panel gap is 2 mm.

Generally, the segment design scheme of the GBT is "small panel" and ensures that the surface accuracy of an antenna with an aperture of hundreds of meters reaches the millimeter scale.

4.1.2. Actuator Design. Every four adjacent segment panels of the GBT share one actuator. The main reflector adopts 2209 precise actuators. A dedicated actuator of the GBT is presented in Figure 5(a); this design greatly cuts down the number of actuators in comparison to a design in which each individual panel is driven by four actuators. It not only reduces the distribution density of actuators and the overall weight of the antenna, but also makes the panels more uniform and more coherent. Therefore, it has good engineering application value. Figure 5(b) shows the mechanical configuration of the GBT actuator [62]. Table 5 presents the design specifications of a GBT dedicated actuator, which uses a "motor screw" with a stroke of 51 cm and achieves a positioning accuracy of 25 μm.

4.1.3. Active Surface Control System and Surface Detection. The GBT active surface control system transmits the antenna deformation information to the master computer via the control bus; the computer subsequently applies the correction data to the corresponding actuator through the control network and control bus to correct the antenna surface shape. All cables connected to the actuators are laid in the cable trough to form a cable network in the back-up structure, which is connected to the control room. The control room is located at the top of the pitch axis, and it accommodates the wiring of all actuators, electronic devices required by control, additional power supplies, and so forth.

For surface detection, GBT adopts out-of-focus (OOF) holography measurement technology [30]. The phase error of the aperture surface is expressed by the Zernike polynomial, and this kind of technology makes a feature of introducing offset focus. The large-scale deformation of large antennas caused by self-weight and temperature at any elevation angle can be measured in real time.

4.2. Large Millimeter Telescope. The LMT adopts active surface adjustment [64], and its surface accuracy reaches 75 μm, which represents the highest precision among all large fully steerable radio telescopes working with the same operating frequency band. It is of great significance in the history of antenna design.

4.2.1. Segment Design. Figure 6 is a segment design diagram of the LMT main reflector, and a hoop/radial annular distribution is also seen on the 50 m paraboloid. Unlike the GBT, it does not depend on other surfaces and is still an intact ring after division into panels. Along the radial direction, the main reflector is divided into five rings composed of a total of five types of panels. Each ring, respectively, contains 12, 24, 48, 48, and 48 panels from inside to outside, so there are 180 combined panels whose positions can be adjusted, as the smallest unit of active surface adjustment. Each panel is made up of 8 high-precision subpanels, and the main reflector of the LMT is composed of 1440 subpanels in total.

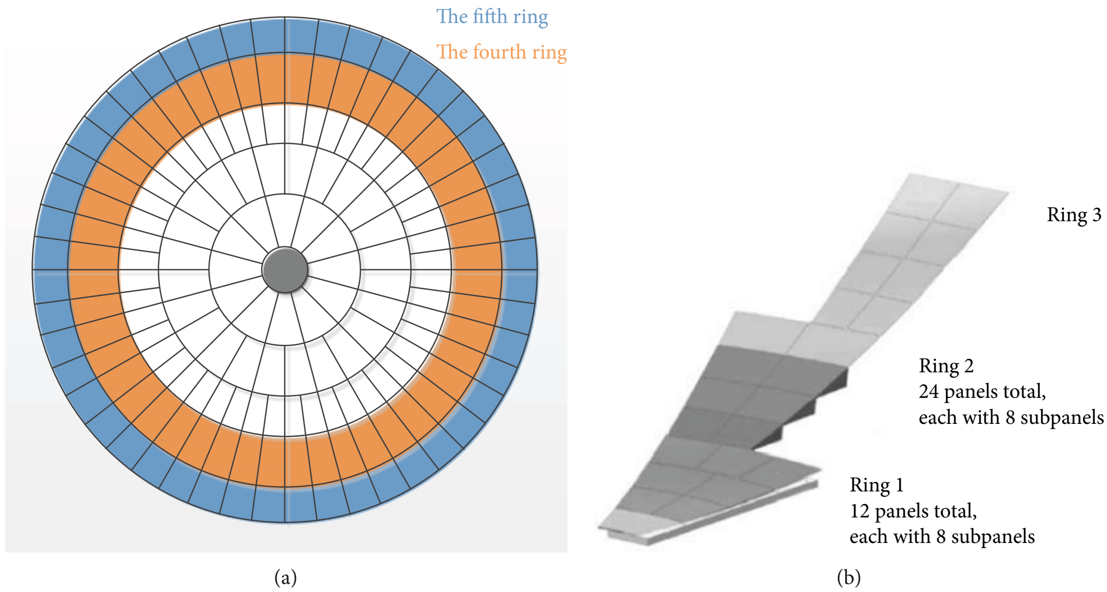

Figure 6: Segment design of LMT main surface. (a) Primary reflector of LMT; (b) panel layout for rings 1, 2, and 3.

A single subpanel is made of an electroformed nickel surface adhered to a honeycomb core made of aluminium whose surface accuracy is 15 μm. At present, only the LMT adopts the design of "combination panels" [65]. Compared to the "small panel" design of the GBT, this method greatly cuts down the number of actuators and effectively reduces the weight of the antenna structure (but the subtruss structure adds extra weight). In addition, it has the advantages of fewer types of panels, easy processing, subpanels with high processing accuracy, as well as easy transportation, and installation. The 25 m CCAT antenna also uses this kind of segment design.

In theory, only three actuators are needed to adjust the position of one panel; however, the combination panel of LMT has large volume and is similar to the shape of a trapezoid, which actually demands more uniform support. Therefore, the form of the "combination panel" adds more support structure, which makes the antenna structure design more complex, and this is an inevitable problem. As shown in Figure 7, the support structure of the combination panel comprises the substrate and subtruss structure. The substrate with high rigidity is riveted together by square section aluminium tube. Through five differential screw adjusting devices, a single subpanel is fixed and regulated with the substrate. The subtruss structure is made of stainless steel and adopts the truss structure that is evenly supported. Through eight balanced supporting points, the whole panel shows uniform stress and deformation under the influence of gravity and presents little deformation.

4.2.2. Actuators and Active Surface Control System. The active surface of the LMT uses a combination panel as an adjustment unit. Four independent precision actuators are adopted to drive and adjust a single panel at its four corners. The LMT altogether employs 720 actuators with a displacement mechanism driven by a DC gear motor, whose positioning accuracy can reach 5 μm. The control network of the LMT is spread over the whole antenna structure, and the control bus is installed with the distribution of each ring of panels. Considering that the numbers of panels in the first, second, and third rings of segment panels are, respectively, 12, 24, and 48, the control bus is divided into 7 groups, each of which is divided into 12 modules to control 12 segment panels individually [64]. Figure 8 shows a configuration diagram of the LMT active surface control system. This method has good scalability, and each bus has an independent AC circuit for easy deployment and promotion.

The active surface control system of the LMT adopts the open-loop control mode, and it controls the movement of the actuators by means of look up table (LUT). Regarding temperature distortion, the LMT structure adopts closed-package handling with positive ventilation in the interior to minimize temperature distortion. In the future, the control of the antenna will be improved through the addition of temperature sensors and related thermal design improvements.

The subreflector of the LMT also uses overall active adjustment. A laser tracker monitors the position of the subreflector. Therefore, the laser tracker can detect the deformation of four secondary support legs or the position offset of the subreflector caused by wind and temperature, and then it transmits a correction signal to the three actuators of the subreflector. Finally, the actuators will move the subreflector to the best position corresponding to the focus of the best-fit paraboloid of the main reflector, which is also an effective compensation method.

4.3. Sardinia Radio Telescope. The active surface adjustment scheme of the SRT is based on the active surface design of a 32 m antenna in Noto, Italy [70, 71], mainly including segment design of main reflector, actuator design, and an active surface control system. The 32 m antenna in Noto was built in 2001, and its overall model had obtained a very good

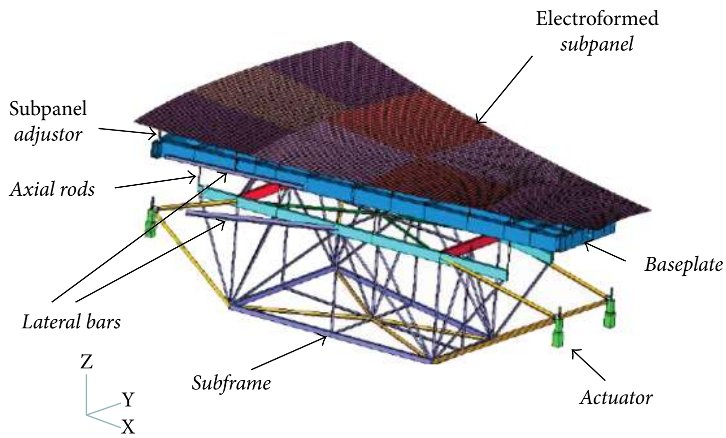

(a)

(b)

Figure 7: Support structure of LMT combination panels [66, 67]. (a) Schematic of LMT segment design; (b) photograph of support structure of an LMT combination panel.

adjustment effect. Valuable experience has been gained through research and application of active surface adjustment of the SRT.

4.3.1. Segment Design. As shown in Figure 9(a), the segment design of the main reflector of the SRT is centrally symmetrical, with a total of 1008 panels distributed along the hoop/radial rings, and the reflector is radially divided into 14 rings. There are 24, 48, or 96 panels in each ring. Referring to Figure 9(b), Table 6 lists the corresponding geometric dimensioning of the panels in the SRT [72]. As with the GBT, the SRT adopts the "small panel" segment design. Each panel consists of an aluminium structural surface and an aluminium Z-type stiffener, whose surface accuracy is better than 65 μm. To obtain such a high-precision panel, the most advanced paste technology in existence in 2006 was adopted. INAF-IRA modified the initial single-panel design of the Vertex RSI Company, so the panel processing precision was enhanced from 0.124 mm to 0.072 mm.

Before active surface adjustment, the surface accuracy of the SRT is 630 μm. When working at the high-frequency band of 23 to 32 GHz, the SRT will start active surface adjustment to compensate for surface deformation caused by gravity, temperature, wind load, and so forth, so the surface precision ranges from 185 to 119 μm. Then the error distributions of gravity deformation, temperature deformation, and wind load deformation are, respectively, 67 μm, 11 μm, and 4 μm (at that time the wind speed is approximately 11.5 kilometers per hour). And at 32 to 100 GHz, SRT is making best effort to improve the surface uniform and feature of antenna main reflector with actuators and different measurement methods.

4.3.2. Actuator Design. Figure 10 is an installation diagram of the SRT actuator. The SRT also adopts the design of "sharing actuators." Four actuators below the four corners of each panel are used for driving and adjusting. A total of 1116 actuators are used for the main reflector.

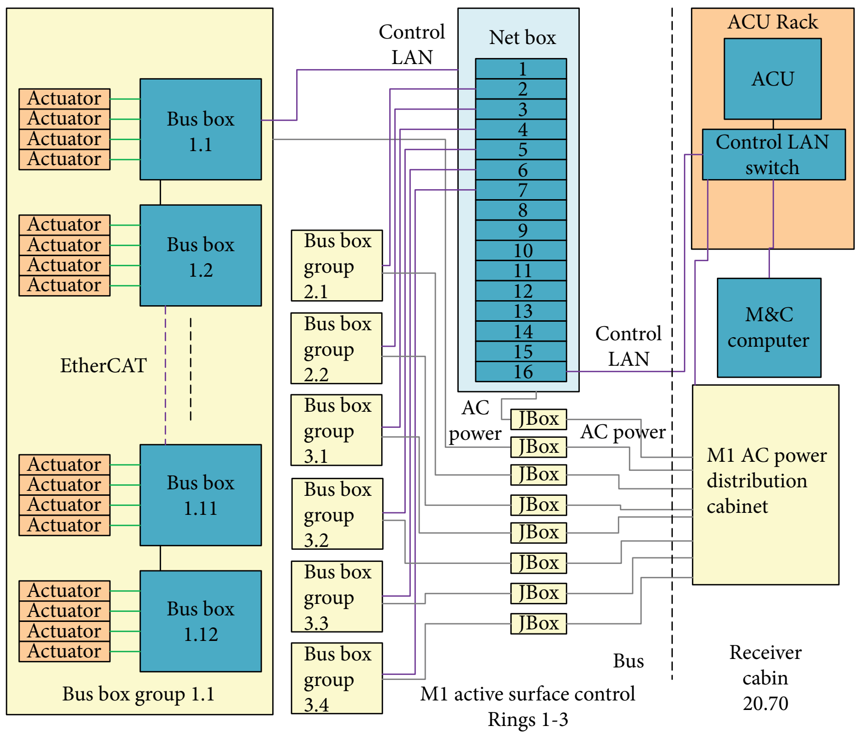

Figure 8: Configuration diagram of the LMT active surface control system [64].

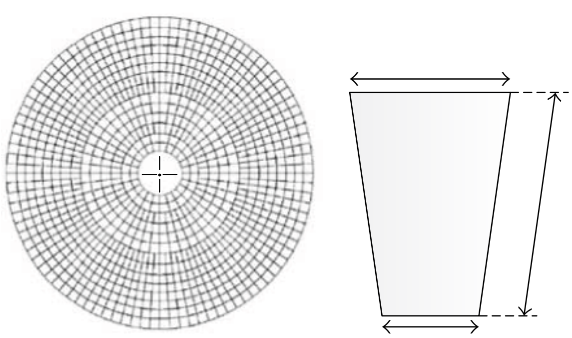

Figure 9: Segment design and panel dimensions of the SRT main reflector [72]. (a) Main reflector of the SRT; (b) geometry of the SRT panels.

Unlike the applications of the first two discussed antennas, the precision actuator of the SRT has two functions: (1) to carry out real-time adjustment of the main surface to make itself close to the ideal surface, reduce the optical path difference of the antenna aperture field, and improve the antenna pointing precision and surface accuracy to compensate the electric performance degradation and (2) to generate the artificial deformation of the main reflector of the antenna for shape transformation between a standard paraboloid and shaped reflector and increase the field of view of the telescope and the highest working frequency of the main focus. These two aims can be summed up as "active homology" and "active deformation," which are also implemented in the actuator function of the QTT. For this purpose, the maximum stroke of an actuator is determined by the larger displacement in two functions. After integration of the design, the stroke of

Table 6: Geometric dimensions of corresponding panels for each ring.

No. ring	C1 (mm)	D1 (mm)	D2 (mm)
1	1670	1214	1646
2	1827	1646	2117
3	2165	1061	1337
4	2166	1337	1611
5	2227	1611	1889
6	2229	1889	2163
7	2313	1082	1221
8	2316	1221	1359
9	2070	1359	1479
10	2073	1479	1597
11	2140	1597	1717
12	2141	1717	1835
13	2241	1835	1956
14	2632	1956	2094

the SRT actuator is 30 mm. The design specifications of the SRT actuators are listed in Table 7 [72].

4.3.3. Active Surface Control System and Surface Detection. The active surface control system of the SRT is an open-loop control system similar that of the LMT, and on this basis, it adds thermal protection and thermal control design, but they have not been installed completely. In addition to photogrammetry measurement and microwave holographic measurement, the antenna design team of the SRT has also studied some more advanced and independent measurement

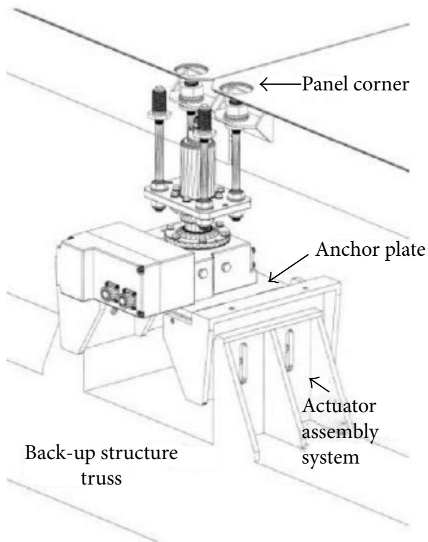

FIGURE 10: Actuator installation of the SRT [68].

TABLE 7: Design parameter specifications of SRT actuators.

Weight	8.5 kg
Specifications	280 mm × 185 mm × 288 mm
Stroke	30 mm
Peak positioning accuracy	±0.015 mm
Axial load	250 kg at work (maximum is 1000 kg)
Radial load	100 kg at work (maximum is 700 kg)
Rate	360 μm/s
Power supply	115 V AC
Communication protocol	RS485 + LAN gateway
Operating temperature range	−10°C/60°C
Min/max power consumption	16/23 VA
Power consumption	4 VA
Service life	20 years

systems, such as linear photoelectric sensors for measuring the deformation of the main reflector and temperature sensors for plotting temperature distribution maps, which are generally made for the most sensitive regions of the radio telescope to predict structural deformations caused by temperature gradients.

4.4. Tianma Telescope. The Tianma telescope is one of the most representative large-scale fully steerable radio telescopes in China, whose working band covers 8 frequency bands, and its surface accuracy is 530 μm before active surface adjustment. During Ka and Q frequency band operation, starting active surface adjustment can make the antenna surface accuracy reach 300 μm, and it shows the corresponding aperture efficiencies of 50% and 45%. As seen in Figure 11, there are four rules that can be summed up: (1) As the operating frequency increases, the antenna efficiency has shown a declining trend when three telescope antennas have the similar aperture sizes. (2) In the case of the same frequency, the antennas with the active surface are more efficient than those without the active surface. (3) Under the circumstance of high frequency, the antenna efficiency of Tianma 65 m with the active surface system not working is sharply reduced compared to itself with the active surface system working. (4) When the two active surface systems of Italy SRT 64 m and Tianma 65 m both work, the antenna efficiencies of these two antennas are quite similar. In addition, with the increase of frequency, the antenna efficiencies decrease slightly but not obviously because of adopting the active surface system. In addition, with the increase of frequency, the antenna efficiencies decrease slightly but not obviously because of adopting the active surface system. In sum, it is known from Figure 11 that the Tianma telescope adopts active surface adjustment when working at a high frequency, which greatly improves the working efficiency of the antenna. At the same time, the Tianma telescope shows higher antenna efficiency than other radio telescopes in the same working frequency [73].

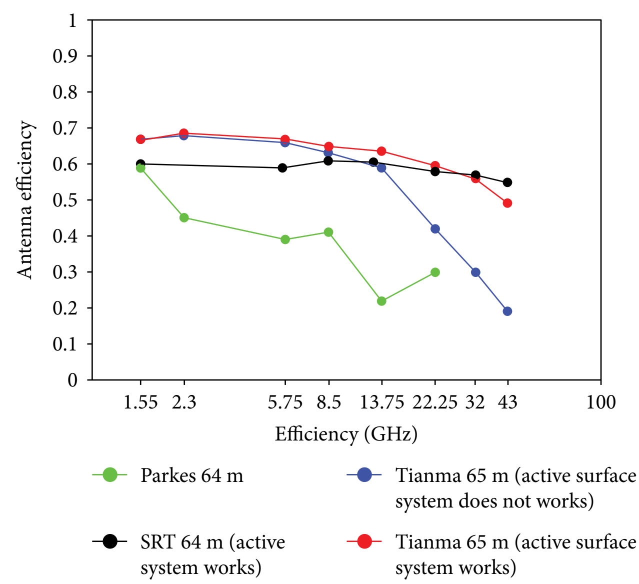

FIGURE 11: Relationship between working frequency and antenna efficiency of the Tianma telescope [69].

4.4.1. Segment Design. The main reflector aperture of the Tianma telescope is 65 m, with the area of 3780 mm^2, which is equivalent to 9 standard basketball courts. It is composed of 14 rings and 1008 individual high-precision solid panels. Its segment design scheme is similar to that of the 64 m antenna of the SRT. The panels from rings 1 to 12 of the Tianma telescope have a surface accuracy of 0.1 mm, and that from rings 13 to 14 of the Tianma telescope is 0.13 mm, which represents the highest level of large-scale panel processing technology in China at that time [74]. The active surface adjustment of Tianma telescope is the first in China. Thus, this large-scale fully steerable antenna is the most advanced design, both domestically and internationally.

4.4.2. Actuators and Active Surface Control System. The actuators of the Tianma telescope are based on the "screw lift"

Table 8: Design parameters of Tianma actuators.

Weight	<13 kg
Height	<330 mm
Stroke	30 mm
Repositioning precision	0.015 mm
Axial load	300 kg (maximum is 1000 kg)
Radial load	150 kg (maximum is 700 kg)
Maximum speed	>0.36 mm/s
Operating temperature range	−10°C/60°C
Service life	20 years

scheme, jointly developed and completed by Nanjing Unid Seiko Technology Co. Ltd. and Shanghai Jiao Tong University. The antenna main reflector is equipped with 1104 precision actuators. Taking the main beams (24 in total) of the antenna back-up frame as a unit, the actuators are divided into 24 groups, with 46 in each group. The actuator has a high positioning accuracy of 15 μm, and it can withstand a lateral load of 150 kg. In addition, the operating life is more than 20 years. The design specifications of the Tianma telescope actuators are listed in Table 8.

Each group of actuators is arranged according to the node distribution of the antenna panel. A rhombic structure is between the actuator and the mounting base, which not only ensures the instalment localization of the actuator, but also prevents torsion of the actuator. Each actuator needs two cables, namely, a power line and a signal line, both of which are fixed on the antenna back-up structure. Each group of actuators is powered in parallel, with a power supply of AC 220 V. The active surface control system adopts the communication method of the distributed bus to implement connection and collaborative work among actuators.

4.5. Summary and Comparisons. The active adjustment technique of the main reflector is applied in the four typical antennas mentioned above, but their active surface design schemes are very different from each other. Through the detailed analysis of the active compensation schemes of the four antennas, the next five aspects are discussed.

(1) For the GBT and SRT, the low working frequency and high working frequency, respectively, correspond to the main focus and the Gregorian focus. The latter occurs when the active surface reflector starts to compensate gravity deformation. In addition, the SRT can adjust the main reflector by means of actuators to realize a shaped reflector, a parabolic reflector, and other surface transformations.

(2) The LMT has the smallest aperture (50 m) among the four antennas, whose main reflector adopts of the unique "combination panel" design. It takes the advantage of finishing machining of the subpanel, which makes the surface accuracy of the main reflector reach 75 μm, so the number of actuators can be greatly reduced. However, on account of the introduction of the subtruss structure, it is difficult to apply it to the antenna structure design with a super-large aperture, such as the QTT, without reducing the complexity of the structure and lightening the back-up structure. The GBT, SRT, and the Tianma telescope all adopt the "small panel" design and shared actuators, thereby reducing the antenna weight.

(3) The SRT and Tianma 65 m are of approximately the same aperture. The former is one of Europe's most powerful telescopes, and the latter was independently developed in China. Although there are some common points in the active surface design of these two antennas, there is still room in China for further development in the field of antenna design, mechanical manufacture, testing, adjustment, and so on, compared with the most advanced technologies abroad. For instance, the main reflector segment of both telescopes adopt the small panel design, and they are divided into 14 rings with a total of 1008 pieces, while for Tianma 65 m, a single segment of the panel has the manufacturing accuracy of 0.1 to 0.13 mm, roughly twice that of the SRT. The adjacent panels share the same actuator for support and adjustment, with a total of 1116/1104 actuators. The actuator stroke and accuracy of the two antennas are very close, while the actuator weight of Tianma 65 m is approximately 1.5 times that of the SRT. To this end, future research should focus of innovation to devise a more lightweight design and improve actuator performance.

(4) At present, the active surface control system and the surface detection method of the four antennas are constantly being improved. Due to the repeatability of self-weight deformation, the four antennas all adopt the LUT open-loop control mode to realize the compensation of self-weight deformation. To eliminate or weaken the influence of solar radiation, the GBT works at night in most cases, and the LMT and SRT use temperature sensors and adopt thermal control measures, while Tianma 65 m in China applies thermal deformation compensation technology. To further improve the efficiency and effectiveness of antenna reflector control, there is still a lot of room for the development of a surface topography acquisition method and a deformation compensation control algorithm.

(5) The four antennas presented above are mainly constructed from traditional materials because of their manufacturing costs and predictability of their elastic modulus and thermal expansion, such as steel and aluminium, while new materials have unlimited potential for application in large antennas. For example, the CCAT antenna, which is being built in the United States, adopts carbon fibre as the main material of the back-up structure, and a composite material is used as the transition of the key connecting

Table 9: Critical performance parameters and design options for QTT.

Major technical parameters	Aperture	110 m
	Work frequency	150 MHz–115 GHz
	Antenna type	Shaped Gregorian
	F/D	0.33
	Surface precision of main reflector	<0.2 mm (when active surface is available) <0.6 mm (when active surface is not available)
	Surface precision of subreflector	<0.07 mm
	Beam pointing precision	<2.5 arcs (when wind speed is 4 m/s)
	Structural weight	Pitching structure < 3000 t Azimuth frame < 2500 t
	Range of pitch angle	7°–89°
	Range of azimuth angle	±270°
Design scheme of actuators	Weight	<10 kg
	Stroke	50 mm
	Positioning accuracy	0.015 mm
	Operating temperature range	−30°C/60°C
Surface detection scheme	Radio holography method	Accuracy: 0.06 mm
	Theodolite method	Accuracy: 1 mm
	Photogrammetric method	Accuracy: 0.04 mm
	Three methods could be adopted simultaneously during observation	
Surface adjustment amount calculation scheme	Electromechanical coupling calculation scheme oriented to beam pointing	According to beam pointing, employ structure deformation information, determine target surface through panel movement and fitting, and show optimal adjustment amount of actuators Adjustment amount database should be set up for quick retrieving.
Active surface control scheme	Closed-loop control with functions of real-time communication, displacement control, real-time feedback, and limit alarm	
	ARM microprocessor and S curve acceleration control algorithm	
	Multithreading control mode software	
Location	Qitai city, Xinjiang province, China at an altitude of 1730–2250 meters	
Time path	The project proposal of QTT was submitted in 2017, and then QTT obtained the approval in Jan 2018. The feasibility study and preliminary design had been carried out for many years, and the construction is expected to build from 2018 to 2023.	

parts and main drive components, to reduce additional losses of the antenna performance due to inconsistent physical properties of the materials. Finally, in the 25 m physical aperture, the CCAT works in the terahertz frequency band with a surface accuracy of 10 μm and no active surface. To improve the antenna performance, the research depth and application range of new materials in ultra-large radio telescopes such as the QTT should be increased.

Among international radio telescopes, the GBT and LMT are, respectively, typical examples of large-aperture and high-precision telescopes. These two antennas were both independently developed in the United States exploiting long history and solid foundation in the field of radio astronomy. To promote the development of astronomical science and deep space exploration technology in China, the QTT should draw more lessons from the successful experiences of foreign antennas in terms of structural innovation design, precision and active compensation, the application of new functional materials, and so on.

5. Proposal for QTT Active Surface Research

Radio telescopes are now being designed to have large apertures, high pointing accuracy, high sensitivity, wide frequency band operation, and large samples. Active surface adjustment has played an important role in addressing the challenges of complex antenna structure and high surface precision. Combined with the above analysis and summary of active surface compensation technologies and the active surface compensation status of international telescopes, the critical performance parameters and design options for the QTT have been determined, and they are shown in Table 9.

In addition, it is recommended for the future construction of the 110 m QTT that the active surface research should focus on the following three aspects:

(1) Segment design of the panel for manufacturing cost and electric performance

The appropriate segment strategy needs to take into account the panel forming process, the switching between the shaped reflector and the standard reflector, and the complexity of the antenna back-up structure. When operating at low frequency, the main reflector is paraboloid, and then it switches to a shaped reflector for the high frequency. In view of the manufacturing capacity of antenna panels in China, the maximum area of a single panel can reach approximately $5\,m^2$, so it is necessary to discuss whether a combination panel should be adopted and how to find a balance between improving the accuracy and keeping the weight. Meanwhile, the error distribution of the panel surface should be determined by the electric performance index (beam pointing and gain). Previous studies by the authors have demonstrated that, while the surface accuracy of total reflector meets the requirements, the antenna may not have the required pointing accuracy. Thus, a reasonable segment of the reflector panels in terms of manufacturing cost and electric performance is an important part in the antenna structure design of the QTT.

(2) High reliability and lightweight of precision actuator

From the foregoing, we can see that the precise adjustment of the reflector must be carried out with an ultra-precise actuator. Further, the assembly of a large number of actuators will inevitably increase the burden of the back-up structure and cause additional perturbation of the main reflector surface, so light weight should be also a key index of the actuator design. Of course, reliability, electromagnetic compatibility, and service life, which are essential factors in the field of the environmental adaptability of all electronic equipment, are necessary considerations for actuator design. In addition, as the number of QTT actuators is expected to reach up to 7600, the manufacturing costs should be decreased by the use of new materials, an integrated process, and outsourced processing.

(3) Development and calculation of accurate active surface adjustment model

With the elevation of the antenna observation, the change of the heat flux of the solar radiation, and the randomness and time-varying nature of fluctuating wind, the deformation of the structure will be uncertain. In addition, the reset accuracy and stroke precision of the actuators, the panel assembly position deviation of the main and secondary reflectors, and the optimum preadjustment angle of panel installation under gravity should be integrated into the active surface adjustment model in different ways. At the same time, a lot of structural detail differences and connection part changes must exist between the finite element model and engineering structure of the antenna reflector and the pedestal structure. Thus, after installation of the antenna, structural mechanics parameter testing (such as local mode shapes) must be conducted, and then the structure finite element model should be gradually modified in detail (for the calculation of panel surface) including revolute joints and degrees of connection freedom. Besides, track unevenness, installation error of the pedestal, and load torsion should be considered and eliminated as a definite error when the antenna beam pointing is being adjusted.

The design and construction of the antenna is not an easy task, let alone various developments of the radio telescope. Along with the larger aperture, the higher frequency, and the more demanding requirements, it will be more difficult. For antenna designers and mechanical engineers, the development and implementation of structure design, pointing control, and active surface adjustment for the ultra-large radio telescope QTT is a long-term and complex process, which is full of opportunities and challenges.

Conflicts of Interest

The authors declare that there is no conflict of interest regarding the publication of this paper.

Acknowledgments

This work was supported by the National 973 Program under Grant no. 2015CB857100, the National Natural Science Foundation of China under Grant nos. 51522507 and 51475349, Youth Science and Technology Star Project of Shaanxi Province under Grant no. 2016KJXX-06, the Fundamental Research Funds for the Central Universities under Grant nos. JBG150409, KJXX1603, and 7214479606.

References

[1] Y. Rahmat-Samii and R. Haupt, “Reflector antenna developments: a perspective on the past, present and future,” *IEEE Antennas and Propagation Magazine*, vol. 57, no. 2, pp. 85–95, 2015.

[2] J. W. M. Baars, “Technology of large radio telescopes for millimeter and submillimeter wavelengths,” *Infrared and Millimeter Waves*, vol. 9, pp. 241–281, 1983.

[3] W. Rusch, “The current state of the reflector antenna art,” *IEEE Transactions on Antennas and Propagation*, vol. 32, no. 4, pp. 313–329, 1984.

[4] B. Du, Y. Wu, Y.-F. Zhang, and G.-X. Liu, “Overview of large reflector antenna technology,” *Radio Communications Technology*, vol. 42, no. 1, pp. 1–8, 2016.

[5] N. Haider, D. Caratelli, and A. G. Yarovoy, “Recent developments in reconfigurable and multiband antenna technology,” *International Journal of Antennas and Propagation*, vol. 2013, Article ID 869170, 14 pages, 2013.

[6] C. Wang, L. Xiao, W. Wang et al., “An adjustment method for active reflector of large high-frequency antennas considering gain and boresight,” *Research in Astronomy and Astrophysics*, vol. 17, no. 5, pp. 4301–4312, 2017.

[7] L.-F. Hao, M. Wang, and J. Yang, “VLBI observations with the Kunming 40-meter radio telescope,” *Research in Astronomy and Astrophysics*, vol. 10, no. 8, pp. 805–814, 2010.

[8] S. von Hoerner, “Design of large steerable antennas,” *The Astronomical Journal*, vol. 72, p. 35, 1967.

[9] W. Gawronski, “Control and pointing challenges of antennas and telescopes,” in *2005. Proceedings of the 2005 American*

Control Conference, pp. 175–178, Portland, OR, USA, June 2005.

[10] B. Y. Duan and C. S. Wang, “Reflector antenna distortion analysis using MEFCM,” *IEEE Antennas and Propagation Magazine*, vol. 57, no. 10, pp. 3409–3413, 2009.

[11] J. W. Mar and H. Liebowitz, “Structures technology for large radio and radar telescope systems,” in *Structures Technology for Large Radio and Radar Telescope Systems*, J. W. Mar and H. Liebowitz, Eds., The MIT Press, Cambridge, MA, USA, 1969.

[12] S. Costanzo, “Reflectarray antennas: analysis and synthesis techniques,” *International Journal of Antennas and Propagation*, vol. 2012, Article ID 945682, 3 pages, 2012.

[13] C. Wang and B. Duan, “On development and application of mechanical-electromagnetic-field coupling model of reflector antennas,” *Acta Electronica Sinica*, vol. 39, no. 6, pp. 1431–1435, 2011.

[14] H. Q. Gan and C. J. Jin, “An optimization of the shape of FAST reflector panels,” *Research in Astronomy and Astrophysics*, vol. 10, no. 8, pp. 797–804, 2010.

[15] N. Li, P. Li, J. Wu, and B. Y. Duan, “Modeling the rail surface unevenness of a high-precision radio telescope,” *Research in Astronomy and Astrophysics*, vol. 17, no. 3, p. 23, 2017.

[16] M. Wang, W. Wang, C. S. Wang, and J. Z. Zhou, “A practical approach to evaluate the effects of machining errors on the electrical performance of reflector antennas based on paneled forms,” *IEEE Antennas and Wireless Propagation Letters*, vol. 13, pp. 1341–1344, 2014.

[17] M. Mobrem, “Methods of analyzing surface accuracy of large antenna structures due to manufacturing tolerances,” in *44th AIAA/ASME/ASCE/AHS/ASC Structures, Structural Dynamics, and Materials Conference*, Norfolk, VA, USA, April 2003.

[18] J. Ruze, “Antenna tolerance theory—a review,” *Proceedings of the IEEE*, vol. 54, no. 4, pp. 633–640, 1966.

[19] B. H. Grahl, M. P. Godwin, and E. P. Schoessow, “Improvement of the Effelsberg 100 meter telescope based on holographic reflector surface measurement,” *Astronomy and Astrophysics*, vol. 167, pp. 390–394, 1986.

[20] P. Zhang, “Structural homology design of large diameter radio telescope,” *Electro-Mechanical Engineering*, vol. 6, pp. 43–46, 2014.

[21] P. Cowles and E. Parker, “Reflector surface error compensation in Cassegrain antennas,” *IEEE Antennas and Propagation Magazine*, vol. 23, no. 3, pp. 323–328, 1975.

[22] S. Xu, Y. Rahmat-Samii, and W. A. Imbriale, “Subreflectarrays for reflector surface distortion compensation,” *IEEE Antennas and Propagation Magazine*, vol. 57, no. 2, pp. 364–372, 2009.

[23] S. Srikanth, *Gain Reduction Due to Gravity-Induced Deflections of the GBT Tipping Structure and Its Compensation*, Technical Report, USA, NRAO, 1994.

[24] J. Q. Wang, L. F. Yu, R. B. Zhao et al., “Sub-reflector model depending on elevations and performance evaluation for TM65 m radio telescope,” *Scientia Sinica Physica, Mechanica & Astronomica*, vol. 44, no. 11, pp. 1232–1240, 2014.

[25] W. Q. Yu and B. J. Shi, “Best-fit of the Cassegrain antenna subreflector and its adjustment,” *Electro-Mechanical Engineering*, vol. 3, pp. 60–71, 1987.

[26] H. Rothman and F. K. Chang, “Maintaining surface accuracy of large radio telescopes by active compensation,” in *Structures Technology for Large Radio and Radar Telescope Systems*, pp. 273–286, Ammann & Whitney Inc., USA, 1969.

[27] A. Greve and H. J. Karcher, “Performance improvement of a flexible telescope through metrology and active control,” *Proceedings of the IEEE*, vol. 97, no. 8, pp. 1412–1420, 2009.

[28] D. R. Smith, K. Souccar, C. A. Magaña, G. Montalvo, and J. L. Hernández Rebollar, “Performance testing of the LMT/GTM primary surface actuators,” in *Advances in Optical and Mechanical Technologies for Telescopes and Instrumentation*, Montréal, Quebec, Canada, August 2014.

[29] C. Sun, L. C. Zhu, and D. J. Yu, “Control algorithm with node movement of the active surface for the FAST,” *Science Technology and Engineering*, vol. 20, no. 3, pp. 489–493, 2012.

[30] Y. Z. Wang, “Design of active surface adjustment system for large radio telescope,” *Radio Engineering*, vol. 40, no. 3, pp. 36–38, 2010.

[31] T. Li, Z. Zhang, A. Li, and Y. Wang, “Active surface control for a large radio telescope,” *Journal of University of Science and Technology of China*, vol. 43, no. 1, pp. 24–28, 2013.

[32] C. Pernechele, C. Barbieri, P. Bolli et al., “A control loop closure system for the Sardinia radio telescope active surface,” in *Proceedings Volume 7739, Modern Technologies in Space- and Ground-based Telescopes and Instrumentation*, San Diego, CA, USA, July 2010.

[33] Z. X. Sun, J. Q. Wang, and L. Chen, “Subreflector model depending on elevation for the Tianma 65m radio telescope,” *Research in Astronomy and Astrophysics*, vol. 16, no. 8, pp. 119–127, 2016.

[34] B. Nikolic, R. M. Prestage, D. S. Balser, C. J. Chandler, and R. E. Hills, “Out-of-focus holography at the Green Bank telescope,” *Astronomy and Astrophysics*, vol. 465, no. 2, pp. 685–693, 2007.

[35] Z. C. Li, G. Y. Li, and X. Y. Wu, “Review of accuracy measuring technology of antenna’s surface,” *Bulletin of Surveying and Mappin*, vol. 6, pp. 16–19, 2003.

[36] D. H. Parker, J. M. Payne, J. W. Shelton, and T. L. Weadon, “Instrument for setting radio telescope surfaces,” in *Proceedings of ASPE 2000 Annual Meeting*, pp. 21–24, Green Bank, WV, USA, October 2000.

[37] L. Y. Li and Y. F. Wang, “Active compensation technology of photoelectric theodolite primary mirror surface-shape error,” *Acta Photonica Sinica*, vol. 42, no. 1, pp. 79–83, 2013.

[38] R. Subrahmanyan, “Photogrammetric measurement of the gravity deformation in a Cassegrain antenna,” *IEEE Antennas and Propagation Magazine*, vol. 53, no. 8, pp. 2590–2596, 2005.

[39] P. Goldsmith, “Resetting the Arecibo primary reflector surface,” *The Arecibo Observatory Newsletter*, vol. 32, pp. 1–4, 2001.

[40] D. M. Gale, “Experience of primary surface alignment for the LMT using a laser tracker in a non-metrology environment,” in *Proceedings Volume 8444, Ground-based and Airborne Telescopes IV*, Amsterdam, Netherlands, September 2012.

[41] J. Bennett, A. Anderson, P. McInnes, and A. Whitaker, “Microwave holographic metrology of large reflector antennas,” *IEEE Antennas and Propagation Magazine*, vol. 24, no. 3, pp. 295–303, 1976.

[42] T. R. Hunter, F. R. Schwab, S. D. White et al., “Holographic measurement and improvement of the Green Bank telescope surface,” *Publications of the Astronomical Society of the Pacific*, vol. 123, no. 907, pp. 1087–1099, 2011.

[43] D. Woody, S. Padin, E. Chauvin et al., “The CCAT 25m diameter submillimeter-wave telescope,” in *Proceedings Volume*

8444, Ground-based and Airborne Telescopes IV, p. 84442M, Amsterdam, Netherlands, September 2012.

[44] J. K. Liang, J. H. Men, Z. T. Ju, and Y. H. Hu, "Microcomputer detection and adjustment system of paraboloid antenna reflector," *Electro-Mechanical Engineering*, vol. 1, pp. 54–60, 1990.

[45] C. Wang, W. Wang, and S. Liwei, *Multifield Coupling Theory and Technology of Microwave Antennas*, Sciences Press, Beijing, 2015.

[46] C. S. Wang, X. Liu, W. Wang et al., "Analysis method of temperature distribution characteristic and thermal distortion of large reflector antennas," *Journal of Astronautics*, vol. 34, no. 11, pp. 1523–1528, 2013.

[47] C. S. Wang, B. Y. Duan, and Y. Y. Qiu, "On distorted surface analysis and multidisciplinary structural optimization of large reflector antennas," *Structural and Multidisciplinary Optimization*, vol. 33, no. 6, pp. 519–528, 2007.

[48] P. Bolli, L. Olmi, J. Roda, and G. Zacchiroli, "A novel application of the active surface of the shaped Sardinia radio telescope for primary-focus operations," *IEEE Antennas and Wireless Propagation Letters*, vol. 13, pp. 1713–1716, 2014.

[49] S. von Hoerner, "Internal twist and least-squares adjustment of four-cornered surface plates for reflector antennas," *IEEE Antennas and Propagation Magazine*, vol. 29, no. 6, pp. 953–958, 1981.

[50] D. Woody, D. MacDonald, M. Bradford et al., "Panel options for large precision radio telescopes," in *Proceedings Volume 7018, Advanced Optical and Mechanical Technologies in Telescopes and Instrumentation*, Marseille, France, July 2008.

[51] C. Wang, B. Duan, F. Zheng, and Y. Qiu, "Mechatronic optimization design and analysis of large space parabolic antennas with active truss support structures," *Acta Electronica Sinica*, vol. 36, no. 9, pp. 1776–1781, 2008.

[52] J. Antebi, F. W. Kan, and R. S. Rao, "Active segmented primary reflector and pointing accuracy of the large millimeter telescope (LMT)," in *Proceedings of SPIE Advanced Technology MMW, Radio, and Terahertz Telescones Conference*, pp. 220–230, Kona, HI, USA, July 1998.

[53] C. S. Wang, L. Xiao, W. Wang et al., "An adjustment method for active reflector of large high-frequency antennas considering gain and boresight," *Research in Astronomy and Astrophysics*, vol. 17, no. 5, p. 043, 2017.

[54] R. M. Prestage, K. T. Constantikes, T. R. Hunter et al., "The Green Bank telescope," *Proceedings of the IEEE*, vol. 97, no. 8, pp. 1382–1390, 2009.

[55] W. M. Irvine, E. Carrasco, and I. Aretxaga, *The Large Millimeter Telescope: Neighbors Explore the Cosmos*, the Five College Radio Astronomy Observatory, USA, 2005.

[56] J. M. Usoff, M. T. Clarke, C. Liu, and M. J. Silver, "Optimizing the HUSIR antenna surface," *Lincoln Laboratory Journal*, vol. 21, no. 1, pp. 83–105, 2014.

[57] O. Hachenberg, B. H. Grahl, and R. Wielebinski, "The 100-meter radio telescope at Effelsberg," *Proceedings of the IEEE*, vol. 61, no. 9, pp. 1288–1295, 1973.

[58] G. Pelosi and G. Tofani, "Sardinia radio telescope (SRT): instrumentation research and development," *IEEE Antennas and Propagation Magazine*, vol. 47, no. 1, pp. 178–180, 2005.

[59] Z. Q. Shen, "Shanghai 65m radio telescope," *Science*, vol. 65, no. 3, pp. 15–20, 2013.

[60] R. D. Nan, "FAST 500m spherical telescope," *Scientia Sinica Physica, Mechanica & Astronomica*, vol. 35, no. 5, pp. 449–466, 2005.

[61] N. Wang, "Xinjiang Qitai 110 m radio telescope," *Scientia Sinica Physica, Mechanica & Astronomica*, vol. 44, no. 8, pp. 783–794, 2014.

[62] R. J. Lacasse, "Green Bank telescope active surface system," NRAO, Kona, HI, USA, 1998.

[63] D. Balser, J. Braatz, D. Frayer et al., *Observing with the Green Bank Telescope*, NRAO, USA, 2015.

[64] K. Souccar, G. Wallace, R. Grosslein, and F. Peter Schloerb, "The architecture of the active surface control system of the large millimeter telescope," in *Proceedings Volume 9151, Advances in Optical and Mechanical Technologies for Telescopes and Instrumentation*, Montréal, Quebec, Canada, July 2014.

[65] M. L. Alvarez, C. T. Torres, E. H. Rios et al., "Metrology and surface adjustment of primary reflector panels on the LMT," in *Proceedings Volume 9151, Advances in Optical and Mechanical Technologies for Telescopes and Instrumentation*, Montréal, Quebec, Canada, July 2014.

[66] D. H. Hughes, J. C. J. Correa, F. P. Schloerb et al., "The large millimeter telescope," in *Proceedings Volume 7733, Ground-based and Airborne Telescopes III*, San Diego, CA, USA, August 2010.

[67] D. Hughes, *The LMT and mmVLBI[C]. From Stars to Black Holes: Mm-VLBI with ALMA and Other Telescopes Scientific Workshop*, ESO, Germany, 2012.

[68] A. Orfei, M. Morsiani, G. Zacchiroli, G. Maccaferri, J. Roda, and F. Fiocchi, "Active surface system for the new Sardinia radiotelescope," in *Proceedings Volume 5495, Astronomical Structures and Mechanisms Technology*, pp. 116–125, Glasgow, UK, September 2004.

[69] Z. Q. Shen, "Tian Ma 65-m radio telescope," in *The 3rd China-U.S. Workshop on Radio Astronomy Science and Technology-Emerging Opportunities*, Green Bank, WV, USA, May 2014.

[70] A. Orfei, M. Morsiani, G. Zacchiroli, G. Maccaferri, J. Roda, and F. Fiocchi, "The active surface system on the Noto radio telescope," in *Proceedings of the 6th European VLBI Network Symposium*, pp. 13–16, Bonn, Germany, June 2002.

[71] G. Zacchiroli, F. Fiocchi, G. Maccaferri et al., "The panels for primary and secondary mirror reflectors and the active surface system for the new Sardinia radio telescope," *Memorie Della Societa Astronomica Italiana*, vol. 10, pp. 126–130, 2006.

[72] E. Cenacchi, *SRT Project Book*, the Istituto di Radioastronomia di Bologna, the Cagliari Observatory (Cagliari) and the Arcetri Astrophysical Observatory (Florence), Italy, 2007.

[73] W. Wang, G. Leng, B. Duan, X. Li, and C. Wang, "Compensation for gravity deformation via subreflector motion of 65 m shaped Cassegrain antenna," *IET Microwaves Antennas & Propagation*, vol. 8, no. 3, pp. 158–164, 2014.

[74] C. Jin, F. Wei, J. L. Li, and H. D. Wang, "Principle and application of precision forming for panel of 65m radio telescope," *Chinese Journal of Radio Science*, vol. 30, no. 1, pp. 1–7, 2015.


Journal of
Engineering
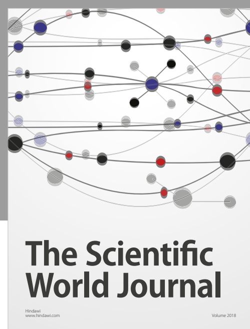
The Scientific World Journal
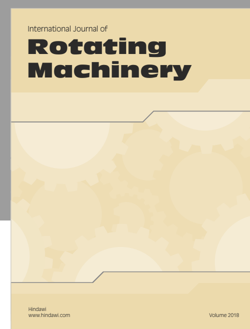
International Journal of
Rotating Machinery

Journal of
Sensors
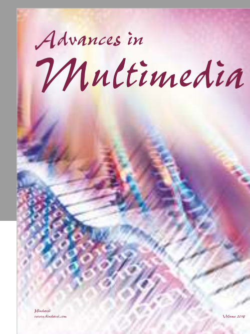
Advances in
Multimedia
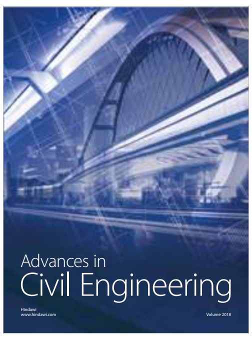
Advances in
Civil Engineering
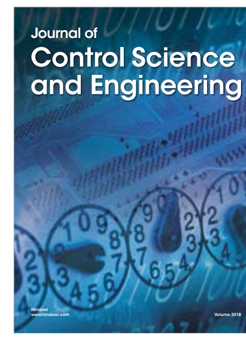
Journal of
Control Science and Engineering


Journal of
Robotics

Journal of
Electrical and Computer Engineering
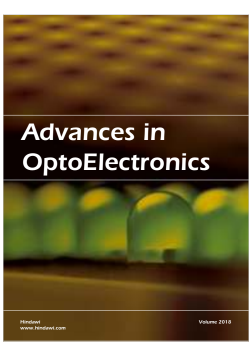
Advances in
OptoElectronics

VLSI Design

International Journal of
Navigation and Observation
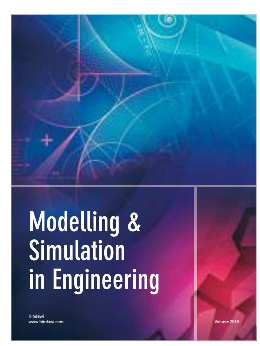
Modelling & Simulation in Engineering

International Journal of
Aerospace Engineering

International Journal of
Chemical Engineering
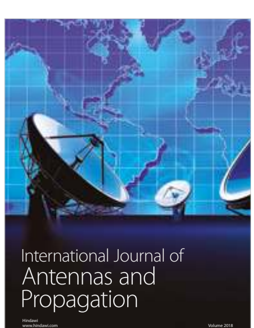
International Journal of
Antennas and Propagation

Active and Passive
Electronic Components
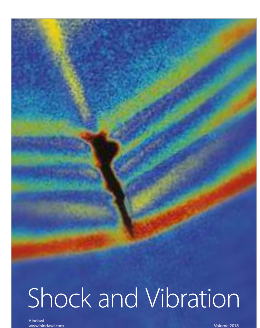
Shock and Vibration

Advances in
Acoustics and Vibration